C_{70} Oxides and Ozonides and the Mechanism of Ozonolysis on the Fullerene Surface. A Theoretical Study

Andrzej Bil,[†] Zdzisław Latajka,[†] and Carole A. Morrison*[,‡]

Faculty of Chemistry, University of Wrocław F. Joliot Curie 14, 50-383 Wrocław, Poland, and School of Chemistry and EaSTCHEM Research School, The University of Edinburgh, King's Buildings, West Mains Road, Edinburgh, EH9 3JJ, U.K.

Received: March 19, 2009; Revised Manuscript Received: June 17, 2009

A series of ab initio calculations have been carried out to determine why the *a,b*- and *c,c*-isomers are the most commonly observed mono-oxides of C_{70} in ozonolysis reactions, when existing calculations in the literature report that these structures are not the most stable conformations. We show that the *a,b*- and *c,c*-isomers are the two most stable structures on the $C_{70}O_3$ potential energy surface, which suggests that the reaction pathway toward oxide formation must proceed via the corresponding ozonide structure. From our calculations, we offer a mechanism for the thermally induced dissociation of $C_{70}O_3$ that share the first two steps with the general mechanism for ozonolysis of alkenes proposed by Criegee. We suggest further steps that involve $C_{70}O_3$ losing O_2 in its triplet or singlet state, thus leaving $C_{70}O$ in its triplet or singlet state, respectively. A pair of products in their singlet states seems to be more likely for the decomposition of *a,b*-$C_{70}O_3$, which ultimately leads to the closed *a,b*-$C_{70}O$ epoxide structure. For *c,c*-$C_{70}O_3$, the more thermodynamically favorable route is the triplet channel, resulting in the triplet open *c,c*-$C_{70}O$ oxidoannulene structure, which may subsequently decay to the singlet ground state *c,c*-$C_{70}O$ epoxide form. This finding offers an alternative interpretation of the experimental observations which reported an open *d,d*-$C_{70}O$ oxidoannulene structure as the metastable intermediate.

I. Introduction

The discovery of oxides of C_{70}[1] in 1991 followed just a few years after the official discovery of Buckminster fullerene (C_{60}) by Kroto et al.[2] Although the number of papers devoted to fullerenes is large, and is growing rapidly, only a very small proportion concerns fullerene oxides. The main achievements in this field have been summarized in two papers by Heymann.[3,4] Fullerenes oxides are usually obtained as products in the synthesis of fullerenes by either electric arcs with graphite electrodes or by low-pressure combustion of hydrocarbons in an oxygen-deficient environment, the latter being the most common route to producing fullerenes commercially. On the laboratory scale they can be synthesized directly by bubbling ozone gas through fullerene solutions, which leads to ozonides, and subsequently fullerene oxides.

Unlike the C_{60} molecule, C_{70} has five nonequivalent carbon atom types (Figure 1), which leads to eight nonequivalent C−C bonds. There are therefore at least eight a priori possible isomers of C_{70} fullerene monooxides, as depicted in Figure 2. The atoms are commonly labeled with letters from *a* to *e*, where *a* refers to apical carbon atoms, *e* labels carbon atoms in the equatorial belt, and *b*−*d* labels the intervening layers. The process of oxide formation may lead to the closed epoxide, where a C−C bond is bridged by an oxygen atom, or it may lead to the open product, a so-called oxidoannulene structure where the C−C bond is broken. In fullerene oxides the orbitals on the carbon atoms attached to the oxygen atom are formally hybridized as sp^3 (epoxide) or sp^2 (oxidoannulene). Although ring puckering even in the case of a bare fullerene can cause hybridization to deviate from pure sp^2, this formal difference has enabled differentiation between fullerene epoxides and oxidoannulenes by ^{13}C NMR spectroscopy.

When $C_{70}O$ was first discovered,[1] it was correctly assumed that the oxygen atom attaches to the external surface of the molecule and bridges two neighboring carbon atoms. The oxidoannulene (open) structure was assumed, although this was subsequently proven to be incorrect. The authors were also not able to recognize which one of the possible isomers had formed. Soon afterwards, several theoretical papers pointed to the *e,e*-$C_{70}O$ open oxidoanullene as being the most stable structure.[5,6] These calculations were performed at the semiempirical MNDO level, as well as at the Hartree−Fock level coupled to the small 3-21G basis set. Similar conclusions were also obtained at the semiempirical AM1 level.[7] On the other hand, other calculations, where the total energy was derived from the sum of an electronic component by the Hückel method and steric contributions from a force field,[8] pointed to isomers *a,b*-$C_{70}O$ and *c,c*-$C_{70}O$ as being the most stable. A further paper[9] [employing classical molecular dynamics (MD) together with single-point semiempirical calculations] also offered evidence in favor of these isomers. It should be emphasized that all these results are obtained at low levels of theory by modern standards and to-date still remain the only sources of theoretical data for these compounds.

The intriguing issue of which isomers are stable and can be synthesized was further highlighted in an experimental paper by Smith et al.[10] Among the products of C_{70} fullerene photooxygenation, two monooxides were isolated, for which UV−vis and ^{13}C NMR spectra were measured. The NMR signals obtained were in the range characteristic for sp^3 carbon atoms and thus supported an epoxide structure for the isomers. The number of lines on the spectra, together with consideration of the symmetry of the molecules, led to a final conclusion that

* Corresponding author. E-mai: C.Morrison@ed.ac.uk.
[†] University of Wrocław.
[‡] The University of Edinburgh.

10.1021/jp9024798 CCC: $40.75
Published on Web 08/17/2009

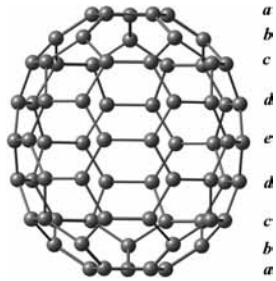

Figure 1. The five different carbon atom environments in C_{70}.

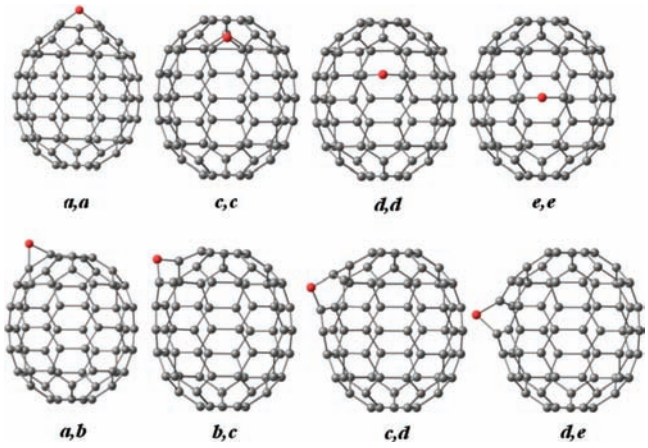

Figure 2. Scheme depicting the eight different possible isomers of $C_{70}O$.

the isomers *a,b*-$C_{70}O$ and *c,c*-$C_{70}O$ were present in the reaction products. Other researchers confirmed by ^{13}C NMR spectroscopy that the same two isomers can be isolated from fullerene soot[11] and are the final products of C_{70} ozonolysis.[12] Their formation has also been reported in the reaction between C_{70} and *m*-chlorperoxybenzoic acid.[13]

Substantial progress on the issue of obtaining new isomers of C_{70} mono-oxides was made by Heymann et al.,[12] where ozonolysis of C_{70} was used to generate the final products. Carried out in the dark, it lead to two mono-ozonides, assigned to be the *a,b*- and *c,c*-$C_{70}O_3$ isomers. Thermal decomposition of the *a,b*-$C_{70}O_3$ molecule lead to the previously known *a,b*-$C_{70}O$ epoxy fullerene, whereas the product of photolysis is the *a,a*-$C_{70}O$ isomer. Interestingly, a second ozonide, *c,c*-$C_{70}O_3$, decays thermally to the *d,d*-$C_{70}O$ oxide, whereas photolysis leads to a mixture of the *b,c*- and *c,d*-$C_{70}O$ forms. Note all of these processes are irreversible. To all four new isomers, the open oxidoannulene structure has been ascribed, on the basis of their UV−vis spectra. All undergo subsequent photoisomerization, giving as final products the two previously known epoxides (*a,b* and *c,c*). The isomers were separated using HPLC, and their transformations were traced by UV−vis spectroscopy alone. None of the new isomers were obtained in a form allowing reliable ^{13}C NMR measurement (the only NMR spectrum that was measured for the isomer ascribed to *a,a*-$C_{70}O$ was of very poor quality). It must therefore be emphasized that the identification of most of the compounds engaged in this complex net of transformations was based on deduction and convincing arguments rather than on ultimate proofs.

To summarize, the problem of the relative stabilities of the eight possible $C_{70}O$ isomers has not yet been resolved. It is unknown why only the *a,b*-$C_{70}O$ and *c,c*-$C_{70}O$ isomers are isolated as final products under laboratory conditions, whereas the results available from theory suggest that these are not the most stable isomers. Others have pointed out that it is not clear whether it is thermodynamic or kinetic factors that determine isomer stability. The aims of this work are therefore to explore these issues by potential energy surface (PES) exploration (minima and transition states optimization) as well as density functional theory (DFT) MD simulation of the parent fullerene and all possible C_{70} mono-oxides and mono-ozonides at room temperature. On the basis of these results, we also propose a mechanism for the thermally induced dissociation of $C_{70}O_3$.

II. Theoretical Calculations

Optimization of all possible structures were performed by using the Becke-Lee−Yang−Parr (BLYP) exchange-correlation DFT functional coupled to a dual localized (Gaussian) and plane-wave basis set description,[14] as implemented in the QUICKSTEP program,[15] which is part of the CP2K suite of software.[16] The localized basis set that was chosen was of double-ζ quality and optimized for use against the Goedecker-Teter-Hutter set of pseudopotentials (incorporated to model the core electrons) and the BLYP functional.[17] The auxiliary plane wave basis set was defined by a cutoff energy of 300 Ry and applied to a cubic periodic boundary condition simulation cell of length 20 Å. The optimized structures obtained were used as starting points for Born−Oppenheimer MD simulations, also run using the CP2K software package with the same basis set and functional description as the one used for the optimizations. The MD simulations were performed in the canonical ensemble (*NVT*), with a time step of 0.7 fs and a chain of Nose-Hoover thermostats to regulate the mean temperature at 298 K. In addition, the TURBOMOLE V5.10 package[18] was applied to pursue optimized geometries corresponding to excited electronic states, to compute IR harmonic spectra,[19,20] and to search for transition-state structures.[21] The basis set used throughout this set of calculations was of double-ζ quality SVP.[22] DFT electronic-structure calculations were performed within the RI-*J* approximation,[23−25] coupled to the BLYP functional. Electronic excitations were calculated by a time-dependent DFT approach.[26] All transition states were unambiguously confirmed by exactly one negative eigenvalue of the Hessian matrix. To confirm that a given transition structure links the product and the reactant, we performed optimization of the structure where changes of geometry followed an eigenvector related to a negative eigenvalue.

III. Results and Discussion

1. Geometry Optimization and Dynamics, C_{70}. Optimized bond lengths obtained for the parent C_{70} molecule are collected in Table S1 (Supporting Information). They support the point expressed in an earlier paper[12] that bonds closer to the equatorial part of the molecule are more aromatic in character than those in the apical part. This stems from two observations: first, that the alteration in bond lengths in the hexagonal *a,a,b,c,c,b* ring is about 0.05 Å, compared to just 0.01 Å for the *d,d,e,d,d,e* ring, and second, that two bonds (*a,b* and *c,c*), found in the apical region, are considerably shorter than the others and possess structural parameters more akin to those of double bonds, rather than aromatic. The MD calculation simulates the behavior of the molecule at room temperature. It was found that all atoms oscillate around the equilibrium structure in such a way that average bond lengths are only slightly longer than those at 0 K (Table S1, Supporting Information).

2. Geometry Optimization and Dynamics, $C_{70}O$. Geometry optimization of all possible C_{70} mono-oxides has confirmed that there are eight main minima on the PES. According to the results

SCHEME 1: Criegee's Mechanism of Ozonolysis

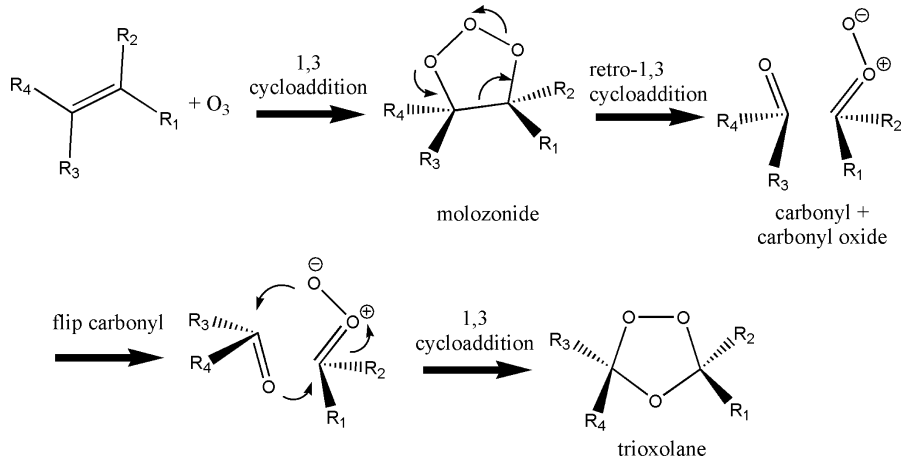

TABLE 1: Total S_0 Energies [kcal mol^{-1}] of the $C_{70}O$ Set of Isomers, Relative to the *a,b*-Isomer, Obtained from Geometry Optimizations (0 K) and Average Potential Energies Obtained from MD Trajectories (298 K)

	0 K	298 K
a,b (ep)[a]	0	0.00 ± 6.38
c,c (ep)	1.25	2.31 ± 7.32
a,a (an)	−2.62	−1.05 ± 6.96
d,d (an)	−2.82	−2.13 ± 6.23
b,c (an)	−0.83	−1.29 ± 5.88
c,d (an)	4.12	5.85 ± 6.02
d,e (an)	10.05	11.88 ± 6.16
d,e (ep)	11.38	–
e,e (an)	−12.82	−12.14 ± 6.10

[a] ep, epoxide; an, oxidoannulene form.

contained in Table 1, the most stable isomer is *e,e*-$C_{70}O$. Two isomers exist as the epoxide form, namely, *a,b*-$C_{70}O$ and *c,c*-$C_{70}O$, whereas all others are oxidoannulenes. This difference may simply reflect the range of C−C bond distances found in the bare fullerene, with the two substantially shorter distances favoring the epoxide structure (Table S1, Supporting Information). In the case of the *d,e* isomer, with a C−C distance in the middle of the range observed, another minimum was revealed that corresponded to an epoxide structure that was slightly higher in energy than the oxidoannulene form. These results confirm suppositions expressed in some earlier papers[5−7] that the *a,b*- and *c,c*- epoxides, which are the only stable compounds under laboratory conditions, are not the ones which would be expected on the basis of the shape of the underlying PES. The difference in total energy between *e,e*-$C_{70}O$ and the other isomers is large enough to confidently make the claim that the *e,e*- form is the definitive global minimum on the PES; this fact is unlikely to alter with further improvements in basis set or level of theory. The differences in energy between the epoxides and the *a,a*-, *d,d*- and *b,c*- oxidoannulenes is however much smaller; further calculation at higher levels may yet result in small differences in the relative ordering of their stabilities.

To understand why the *a,b*- and *c,c*- epoxide structures are favored above all others, it is therefore necessary to go beyond the basic geometry optimized (0 K) calculation. The next step is to compute zero-point energy (ZPE) corrections for all isomers, and this was done on the basis of their harmonic vibrational spectrum. It was found that the molecular vibrations at 0 K do not exert much influence on the relative stability of the series of isomers, because all ZPE correction values fall within a narrow range, from 276.81 kcal mol^{-1} for *d,e*-$C_{70}O$ to 277.43 kcal mol^{-1} for *e,e*-$C_{70}O$.

Because the energies related to the minima on the PES determine the thermodynamical stability of the isomers at 0 K, the shape of the PES in the vicinity of these points will also influence the properties of the isomers at higher temperatures. To investigate how C_{70} oxides under laboratory conditions may explore the nonequilibrium parts of the PES, we have also performed MD simulations. We were able to obtain a trajectory for each isomer in the range of 3 ps. The average potential energies, together with energy fluctuations, were estimated by using a standard application of the blocking method[27] and are collected in the second column of results presented in Table 1. The main effect of providing a thermal stimulus is to increase the energy in the range from 59.5 kcal mol^{-1} (*b,c*-$C_{70}O$) to 61.8 kcal mol^{-1} (d,*e*-$C_{70}O$). As the value is very similar for the whole set of isomers, the thermal factor is not expected to change their relative stabilities, at least in the vicinity of the temperature applied in these simulations. Thus, the calculations performed so far have not provided an explanation as to why the *a,b*-$C_{70}O$ and *c,c*-$C_{70}O$ isomers are favored under experimental conditions.

Turning now to consider molecular geometries, Table S2, Supporting Information, contains distances between the carbon atoms to which the oxygen atom is attached. The C−C bond length in the *a,b*- and *c,c*-epoxy-fullerenes is only slightly longer than that typically ascribed for bonds between two sp^3 atoms. The presence of the oxygen atom elongates the bond by about 0.15 Å compared to the bare fullerene (Table S1, Supporting Information). The distance between carbons for those isomers existing in the oxidoanullene form exceeds 2 Å, reaching even 2.26 Å for the equilibrium structure of the *e,e*-isomer, which is far greater than the length typically ascribed to a double or even single C−C bond. It can therefore be concluded that the chemical bond between carbon atoms in this type of structure has been severed. Applied thermal excitation influences the C−C distance only slightly, leading to average values no longer than 0.01 Å compared to the equilibrium values.

An average C−C bond distance value shorter than the equilibrium value, as observed for *d,e*-$C_{70}O$ [298 K 2.11(14) Å, 0 K 2.16 Å], needs an explanation. As mentioned above, the equilibrium structure for the *d,e*-isomer takes the oxidoannulene form, but this minimum is accompanied on the PES by an epoxide structure that is only slightly higher in energy and possesses a C−C bond that is much shorter (1.58 Å). The range covered by the minimal and maximal distances observed during the MD simulations proves that both wells on the PES are

TABLE 2: Total S_0 Energies [kcal mol^{-1}] of the $C_{70}O_3$ Set of Isomers, Relative to the *a,b*-Isomer, Obtained from Geometry Optimizations (0 K) and Average Potential Energies Obtained from MD Trajectories (298 K)

	0 K	298 K
a,b	0	0.00 ± 6.32
c,c	2.33	2.02 ± 5.95
a,a	15.72	15.44 ± 8.77
d,d	5.43	4.62 ± 6.65
b,c	12.31	12.24 ± 6.85
c,d	16.54	16.00 ± 7.15
d,e	13.65	13.92 ± 6.93
e,e	30.72	29.34 ± 7.05
e,e (dis)[a]	19.22	18.76 ± 6.21

[a] Product observed in the spontaneous ring-opening reaction recorded in the MD trajectory for *e,e*-$C_{70}O_3$.

sampled, and thus, more of the PES is explored for this isomer than for the others, which is also reflected in the larger standard deviation for this distance compared to that observed for the other members of the $C_{70}O$ series (Table S2, Supporting Information). The 298 K average value is, however, closer to the oxidoannulene equilibrium distance than the epoxide, which means that this structure dominates. In fact, extending the simulation to 5 ps allowed the oxide to switch to the epoxy-structure just once, and it remained in the vicinity of this minimum for a short time only. Thus, for the *d,e*-$C_{70}O$ isomer, interpretation of a ^{13}C NMR spectrum may be complicated by the fact that signals from the C_d and C_e atoms are likely to be more upfield than other signals typical for sp^2 atoms. But in short, the question of whether a second minimum really exists for the *d,e*-isomer is of minor importance, because it relates to small details on the PES, which may be strongly dependent on the choice of basis set or functional.

3. Geometry Optimization and Dynamics, $C_{70}O_3$. As the thermal stimulus does not influence considerably the relative stabilities of the $C_{70}O$ isomers, other factors must be responsible for the fact that the most thermodynamically preferable product has never been observed. Because the oxides are formed by decomposition of ozone-bridged C_{70} compounds (so-called molozonides), the shape of the PES for ozonides may play the key role. Such a point of view has been expressed in previous theoretical papers.[7,9] Table 2 presents the total energies of all possible ozonides in relation to the *a,b*-$C_{70}O_3$ isomer. The most notable feature of this PES is its entire difference from the one obtained for the oxides. First of all, the *a,b*- and *c,c*-$C_{70}O_3$ isomers are the most stable; the energies of the other isomers, (including *e,e*-), are considerably higher. It is perhaps then not so surprising that only isomers *a,b*-$C_{70}O_3$ and *c,c*-$C_{70}O_3$ were recognized in the experiments by Heymann.[12] The large value of the total energy of the *e,e*-isomer, which is the largest of the series and considerably greater than the energies of other less likely isomers, seems to serve as a good explanation for the fact that experimentally the *e,e*-$C_{70}O$ molecule remains unknown. Thus, we conclude that the most stable oxide cannot be obtained, because it would have to originate from the least thermodynamically probable ozonide.

Addition reactions, which occur by opening up the double bond, should lead to a lengthening of the C−C distance. Indeed, C−C bonds in the vicinity of an ozone bridge in most ozonides are longer than those in the bare fullerene by about 0.2 Å (cf. Tables S3 and S1, Supporting Information). In the case of *e,e*-$C_{70}O_3$, this change is as much as 0.27 Å, which leads to a C−C distance of 1.76 Å. This value may suggest that the bond is close to its dissociation point, which may give an explanation as to why the energy of this isomer is considerably higher than the others.

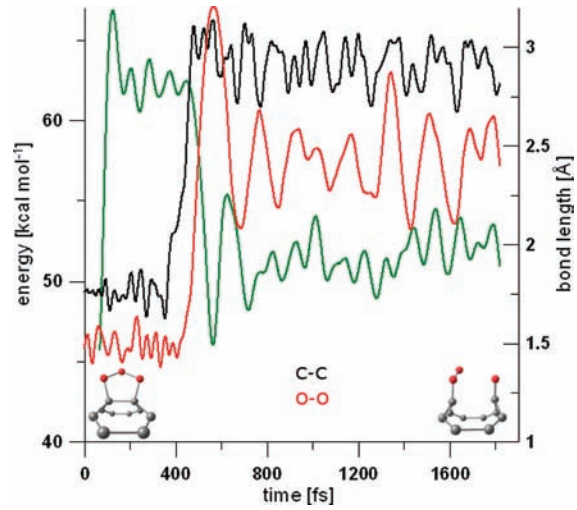

Figure 3. Selected parameters obtained from a section of the MD run performed for *e,e*-$C_{70}O_3$. The bond lengths C−C (black) and O−O (red) as well as the potential energy (green) are depicted versus simulation time.

To make sure that the conclusions derived from the shape of PES remain valid in nonzero temperature conditions, we also performed an MD study for the fullerene ozonides. As in the case of oxides, the simulations were long enough to obtain trajectories of around 3 ps in duration. The average potential energies of all isomers and the energy fluctuations were estimated using the blocking method; results are collected in Table 2. It is noted that the thermal boost for all molecules is of the order of 63 kcal mol^{-1} and therefore does not directly influence the relative stability of the ozonide series. During the MD simulation, the *e,e*-$C_{70}O_3$ isomer underwent a chemical reaction, which will be discussed in more detail in the following section.

Turning the discussion back to molecular geometries, the average C−C bond lengths observed in the MD simulation runs for the $C_{70}O_3$ series (Table S3, Supporting Information) are only slightly longer than equilibrum ones. It appears that, apart from the *e,e*-isomer, the thermal motion of atoms does not lead to qualitative changes in molecular structures.

A typical feature of an alkene is its ability to react in many addition reactions. The shape of the PES of the ozonides is in agreement with previously expressed conclusions, namely, that the *a,b* and *c,c* bonds in the C_{70} cage share some double-bond character.[12,28] It therefore follows that the *a,b*-$C_{70}O_3$ and *c,c*-$C_{70}O_3$ isomers might be expected to be the most obvious candidates for products as a consequence of ozone addition. Indeed, our calculations prove that these isomers are the most stable. However, there is no straightforward connection between bond length (i.e., double-bond character) and the thermodynamical stability of the product. Although the *c,c* bond is slightly shorter than *a,b* in the bare fullerene, it is the *a,b*-$C_{70}O_3$ isomer which is the most stable product on the PES. Moreover, the *d,e*-$C_{70}O_3$ isomer has a much higher total energy than the *d,d* one, despite possessing the shorter C−C bond.

4. Proposed Mechanism for the Dissociation of $C_{70}O_3$. An MD simulation of *e,e*-$C_{70}O_3$ leads to the spontaneous dissociation of the C−C bond, as well as one of the O−O bonds. Bond lengths and the total energy of the system are depicted as a time function in Figure 3. Energy is expressed in relation to

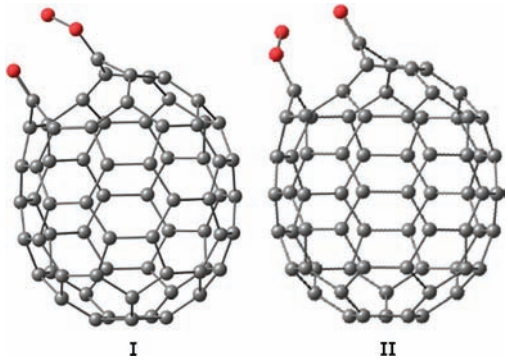

Figure 4. Isomeric products (I, II) of the ring-opening reaction observed for *a,b*-$C_{70}O_3$.

the initial equilibrium structure. During the system equilibration, the molecule oscillates around the equilibrium structure. After ca 350 fs, the C−C bond dissociates, with the bond length increasing from 1.63 to 3.11 Å over the course of 130 fs. This action triggers the dissociation of an O−O bond some 53 fs after the C−C bond starts to dissociate. This bond increases from 1.43 to 3.21 Å. Thus, the reaction leads to a structure where a single oxygen atom is attached to one *e*-type carbon atom, and an O_2 molecule is attached to the second one. In further steps of the dynamics, the system oscillates around this new minimum, with the O_2 unit swinging round relatively freely. The average value $C_e\cdots C_e$−O−O torsion angle is about 75° with a statistical uncertainty as large as 12°. As is clear from the potential energy line shown in Figure 3, the dissociation leads to a new structure which is more stable than the initial one.

Subsequent optimization of the dissociated form of the *e,e*-isomer (labeled as *e,e*-$C_{70}O_3^{(dis)}$ in Table 2 and Table S3, Supporting Information) leads to a minimum which is only 19.22 kcal mol^{-1} less stable than our reference point (*a,b*-$C_{70}O_3$) and therefore some 11.50 kcal mol^{-1} more stable than the nondissociated *e,e*-$C_{70}O_3$ (Table 2). Interestingly, this observed process is in line with the general mechanism of ozonide formation and decomposition proposed some thirty years ago by Criegee[29] and subsequently confirmed by isotope studies.[30] The first step involves addition of an ozone molecule to a C−C double bond which leads to the formation of a molozonide (Scheme 1). Next, the breaking of the C−C and O−O bonds results in carbonyl and carbonyl oxide structures. This is then followed by a carbonyl flip to lead to an intermediate from which a 1,3-cycloaddition process leads to the formation of trioxolane. Subsequent reduction of this gives aldehydes or ketones as the final products. Our simulation shares the C−C bond breaking, followed by O−O bond dissociation steps highlighted in this mechanism.

As the dissociation of the *a,b*- and *c,c*-ozonide isomers has been proven experimentally, we assumed that the mechanism of these reactions would be similar to the one we had observed for the *e,e*-isomer and proceeded to search for transition-state structures. Due to the symmetry of the *c,c*-$C_{70}O_3$ isomer, both O−O bonds are equivalent; thus, only one product of ring-opening is possible. In the case of the *a,b*-$C_{70}O_3$ reactant, two isomeric products are possible, as depicted in Figure 4. Both structures have almost the same energy, with structure I the more stable of the two by just 0.03 kcal mol^{-1}. The transition state linking the reactant with structure II is only 0.14 kcal mol^{-1} higher in energy than that connected with product I.

The energy profile obtained for the ring-opening reaction for *a,b*-$C_{70}O_3$, along with associated structures, is presented in Figure 5; the results for the *c,c*-isomer are in Figure 6. Note that the points on the graph represent geometries that were generated from the transition-state structure following an eigenvector of the Hessian matrix related to the negative eigenvalue. It should be stressed that the reaction pathways found for the dissociation of the *a,b*- and *c,c*-ozonide isomers are qualitatively different from that observed spontaneously for the *e,e*-$C_{70}O_3$ isomer in the MD simulation. In the case of the *c,c*-isomer, the energy difference between reactant and product is about 11.77 kcal mol^{-1}, whereas for the *a,b*-isomer it is only 5.78 kcal mol^{-1}. The reaction barriers are 14.94 and 11.95 kcal mol^{-1}, respectively. As stated previously, the thermal boost from the MD calculations leads to average potential energies being about 63−64 kcal mol^{-1} higher than those for the 0 K structure, which is about 0.86 kcal mol^{-1} per atom. This value is comparable to the reaction barrier calculated for the *e,e*-isomer (0.7 kcal mol^{-1}) and much smaller than the barriers calculated for the *a,b*-and *c,c*-isomers, which means that dissociation is unlikely to be observed in an MD run for the latter isomers at the temperatures employed in these simulations.

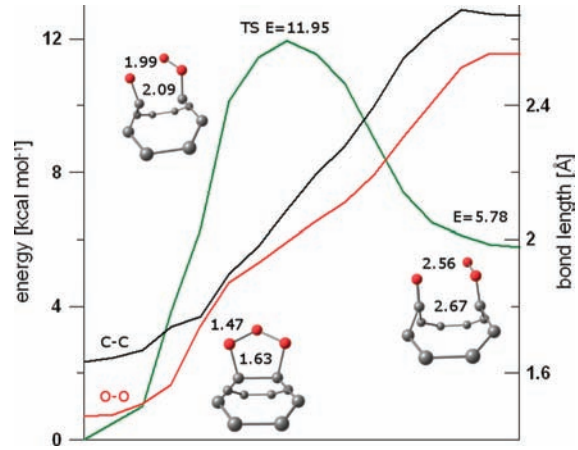

Figure 5. Calculated energy profile (in green) for the *a,b*-$C_{70}O_3$ ring-opening reaction, leading to the product *a,b*-$C_{70}O_3^{(dis)}$(I). Changes in bond lengths observed for C−C and O−O are given in black and red, respectively.

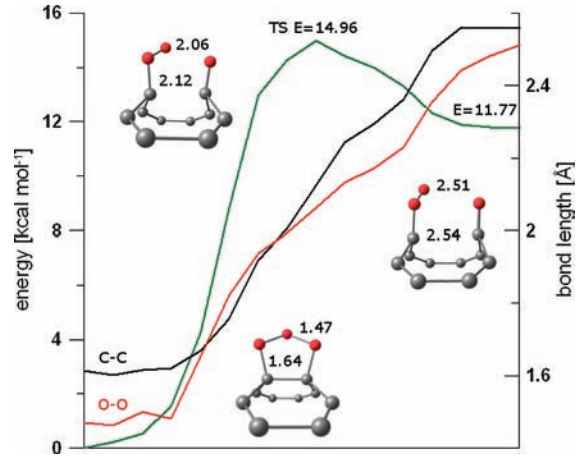

Figure 6. Calculated energy profile (in green) for the *c,c*-$C_{70}O_3$ ring-opening reaction. Changes in bond lengths observed for C−C and O−O are given in black and red, respectively.

Some improvement to reaction energy barriers can be obtained by introducing a component of pure Hartree−Fock exchange to the density functional,[31−33] which leads to much more computationally demanding hybrid functionals, such as B3LYP. For the *a,b*- and *c,c*-isomers a series of single-point

TABLE 3: Calculated Energy Barriers and Estimated Experimental Activation Energies (kcal mol^{-1}) for the Ozone Ring-Opening Reactions for Isomers *a,b*-$C_{70}O_3$ and *c,c*-$C_{70}O_3$

	a,b-$C_{70}O_3$ → *a,b*-$C_{70}O_3^{(dis)}$(I)	*a,b*-$C_{70}O_3$ → *a,b*-$C_{70}O_3^{(dis)}$(II)	*c,c*
BLYP	11.95	12.09	14.96
B3LYP	20.80	20.94	24.30
Exp.[a]	22.6	−	24.4

[a] From ref 12.

TABLE 4: Calculated Molecular (*r*, Å) and Electronic (*q*) Parameters of the Products of Molozonide Ring-Opening in the *a,b*-, *c,c*-, and *e,e*-Isomers of $C_{70}O_3$

	a,b-$C_{70}O_3^{(dis)}$(I)	*a,b*-$C_{70}O_3^{(dis)}$ (II)	*c,c*-$C_{70}O_3^{(dis)}$	*e,e*-$C_{70}O_3^{(dis)}$
C═O				
*r*C═O	1.22	1.22	1.22	1.24
q C	0.50	0.50	0.48	0.47
q O	−0.45	−0.44	−0.45	−0.42
C═O−O′				
*r*C═O	1.30	1.31	1.31	1.33
*r*O−O′	1.34	1.35	1.34	1.35
q C	0.40	0.40	0.39	0.38
q O	−0.08	−0.09	−0.09	−0.11
q O′	−0.27	−0.27	−0.26	−0.23

energy calculations using the B3LYP functional were performed for the reactants and transition states (which were previously optimized using the BLYP functional). The results are collected in Table 3, where it is immediately apparent that the introduction of exact Fock exchange has resulted in barrier heights increasing by a factor of nearly two, bringing the simulation into very close alignment with experiment.[12] Our results also predict that the reaction barrier for the *c,c*-isomer will be higher than that for the *a,b*-form, which again finds close agreement with experimental measurements.[12]

Further steps of the reaction taking place on the surface of the C_{70} cage remain unknown. It is obvious, however, that the rest of the mechanism must be different from the one proposed by Criegee. First of all, the reaction leads to an oxide and O_2 as the final products rather than a trioxolane. The fullerene cage is stiff which protects the carbonyl oxide (C−O_2) functional group from flipping. Furthermore, formation of trioxolane would lead to an endohedral positioning of an oxygen atom, which is unlikely from an energetic point of view. Indeed, a test calculation performed for the *c,c*-isomer confirmed that the trioxolane arrangement, although a stable minimum on the PES, is 49.8 kcal mol^{-1} higher than the total energy for the molozonide form.

Table 4 lists some calculated parameters that characterize the bonding in the products observed in the ring-opening reaction of the C_{70} ozonides. According to the Criegee mechanism, a single oxygen atom attached to a carbon atom should form a carbonyl group. This is supported by the simulations: calculated bond lengths in all products are short, which is indicative of a double-bond structure, and the NPA (natural population analysis) atomic charges, *q*,[34] indicate large charge separations. For the C−O_2 group (see Scheme 1), distances between the C and O atoms are longer, indicating that these bonds are more likely described by a single/double-bond resonance structure, as proposed in Scheme 2a. The NPA charges in this group indicate that there is a shift in the electron density, leading to a large positive charge on the C atom and a negative charge on the terminal oxygen atom, whereas the interior O atom is left almost unaffected.

SCHEME 2: (a) Proposed Resonant Structures for the Products of the Ozonide Ring-Opening Reaction and (b) a Possible Mechanism for the Formation of the Closed Oxide Structure

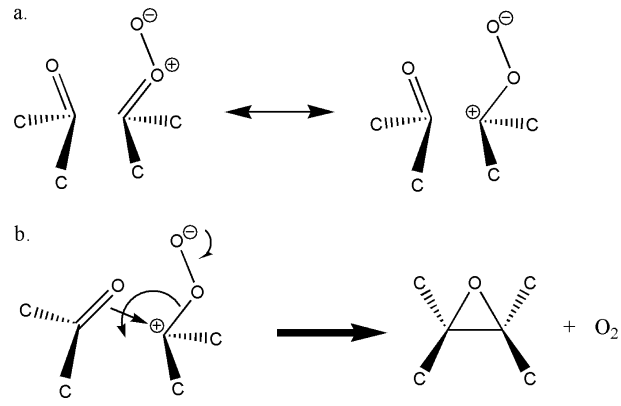

Our calculations suggest that the opening of the ozonide ring in the *a,b*-$C_{70}O_3$ molecule leads to two isomers which are equally probable. Both of them must ultimately lead to the epoxide product *a,b*-$C_{70}O$, because thermolysis of this ozonide results in only one detectable product. This strongly suggests that the next step of the reaction is connected exclusively with the formation of an oxygen bridge over a C_a—C_b bond that forms simultaneously. By using the above-mentioned resonant structures, we propose a mechanism for this process which is depicted in Scheme 2b. This process should be favorable because it does not influence the existing net of C—C bonds in the fullerene cage. Note that if the oxygen bridge were to form with another atom adjacent to C_a or C_b (i.e., C_a—C_a or C_b—C_c), this would lead to an annulene structure.

As the same mechanism of thermolysis can be expected for *c,c*-$C_{70}O_3$, it is surprising that it has been reported to lead exclusively to the transient *d,d*-$C_{70}O$ isomer.[12] There is no clue allowing us to explain this experimental phenomenon on the basis of the calculations performed thus far. It should be emphasized, however, that it is not clear whether the O_2 molecule is initially released from the $C_{70}O_3$ unit in its electronic singlet or (more stable) triplet state. Due to complex electronic structure, C_{70} (as well as its oxides and ozonides) is expected to have relatively low-lying electronic excited states. As the difference in energy between the singlet and triplet oxygen molecules is only about 22.5 kcal mol^{-1}, considering the shapes of the PESs of the $C_{70}O$ isomers referring to their triplet state may be crucial to understanding the chemistry taking place on the fullerene surface.

As mentioned earlier, in their S_0 states, the *a,b*-$C_{70}O$ and *c,c*-$C_{70}O$ isomers have only one minimum, referring to closed epoxide structures, with C_a—C_b and C_c—C_c distances of 1.57 and 1.55 Å, respectively. Interestingly, we have found that, on the T_1 PESs, there are two minima. The first again refers to the closed epoxy structures, while the second, and more stable minima, refer to the open oxidoannulene structures, with C_a—C_b and C_c—C_c bond distances of 2.24 and 2.20 Å, respectively.

For ease of reference, we list symbolically in Figure 7 the structures related to *a,b*-$C_{70}O_3$ and its possible products of decomposition on a common energy scale. Structure 1 is the optimized (equilibrium) structure of *a,b*-$C_{70}O_3$. As mentioned above, this structure passes through a transition state (structure 2) resulting in the ozonide ring-opening to give rise to a new, lower-energy structure (structure 3). Structure 4 refers to the open oxidoannulene *a,b*-$C_{70}O$, which is a minimum on the T_1

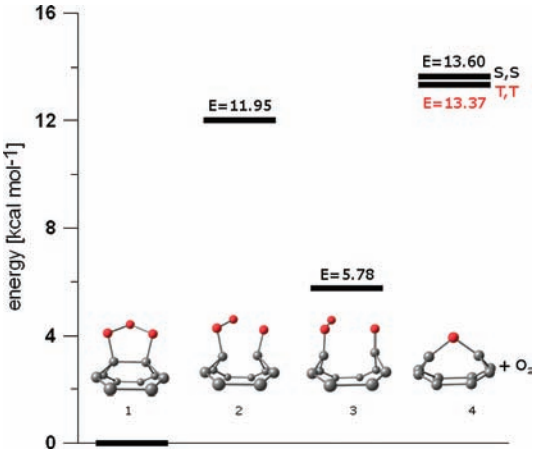

Figure 7. Characteristic points on the decomposition pathway of *a,b*-$C_{70}O_3$. Structures 1 and 3 represent minima, 2 is a transition state on the S_0 PES, and 4 is a minimum on the T_1 PES of *a,b*-$C_{70}O$.

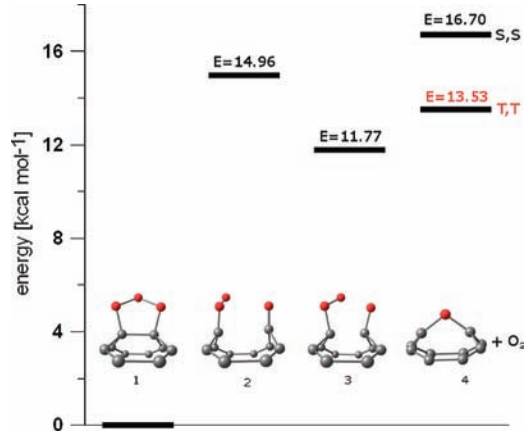

Figure 8. Characteristic points on the decomposition pathway of *c,c*-$C_{70}O_3$. Structures 1 and 3 represent minima, 2 is a transition state on the S_0 PES, and 4 is a minimum on the T_1 PES of *c,c*-$C_{70}O$.

PES, together with the triplet O_2 molecule (i.e., the T,T path, where structure 3 dissociates giving both $C_{70}O$ and O_2 in their triplet electronic states). We have also marked the total energy of the structure with the same geometry but possessing the singlet ground electronic state, together with the singlet oxygen molecule (i.e., the S,S path). Note that because our theoretical model is not subject to any external perturbation (e.g., solvent, temperature, or interactions with other molecules in solution) that could give rise to electronic relaxation, our calculations must observe the spin-conservation principle, such that a molecule must dissociate to create a pair of products with the same overall spin state as that of the parent molecule. The conclusion to be drawn from Figure 7 is that the T,T and S,S dissociation channels have very similar total energies and theoretically are equally probable. However, it is known from experiment that the *a,b*-$C_{70}O_3$ ozonide decomposes to a closed epoxide structure.[12] This supports the S,S path of dissociation from structure 3.

The analogous set of structures for the *c,c*-$C_{70}O_3$ isomer are presented in Figure 8. Once again, structure 4 refers to the open oxidoannulene *c,c*-$C_{70}O$, which is a minimum on the T_1 PES, together with the triplet O_2 molecule. Their S,S counterparts (with a total energy derived from single-point energy calculations corresponding to the triplet geometries but with singlet electronic structure arrangements) are higher in energy, which suggests that for this isomer, the T,T dissociation channel may be more favorable than the S,S one. Our calculations therefore suggest that the most likely initial product for the decomposition of *c,c*-$C_{70}O_3$ is the open oxidoannulene *c,c*-$C_{70}O$ in its triplet state. An experimental study[12] of the thermoloysis pathway of *c,c*-$C_{70}O_3$ quotes a surprising observation that the resulting product is a metastable structure, the UV−vis spectrum of which shares features characteristic for open oxidoannulenes. Because of this, the authors ascribed the structure to be *d,d*-$C_{70}O$, which does indeed adopt the oxidoannulene form (Table S2, Supporting Information), but requires a rather complicated mechanism of formation, involving transfer of an O atom from a C_c-C_c bond to a C_d-C_d bond.

In assessing the likely credibility of the T,T dissociation channel, the properties of the C_{70} molecule in its lowest-lying triplet state should be mentioned.[35,36] It is reported that the intrinsic triplet lifetime of C_{70} at room temperature in toluene solution is at least 11.8 ms, which is 83 times longer than that of C_{60}.[36] The authors of this study also state that the concentration-dependent triplet kinetics of C_{70} are surprisingly complex, with their data strongly suggesting the formation of triplet excimers via a pair of triplet and ground state C_{70} molecules. We think that similar behavior is not unlikely in the case of C_{70} oxides, although, to our knowledge, no experiment has been reported to measure the triplet lifetimes of C_{70} oxides. Because the oxides are slightly polar, the influence of solvent on triplet kinetics might be even more important here than for the bare fullerene. Interestingly, the metastable fullerene oxide ascribed to be *d,d*-$C_{70}O$[12] is reported to photoconvert with very high efficiency to *c,d*-$C_{70}O$ and then to *c,c*-$C_{70}O$. No quantitative data are, however, available.

It seems, therefore, that the nature of formation of *c,c*-$C_{70}O$ from *c,c*-$C_{70}O_3$ remains unknown and is more complicated than was expected. Hypothetically, if we assume that structure 3 (Figure 8) dissociates by following the more energetically favorable T,T channel, the metastable product is *c,c*-$C_{70}O$, but in its triplet electronic state, and therefore has an open oxidoannulene structure, in agreement with the measured UV−vis spectrum. This metastable structure sits some 13.53 kcal mol^{-1} above the S_0 *c,c*-$C_{70}O$ closed epoxide structure, to which it may well eventually decay to through a net of complicated processes induced by molecular collisions, as observed for the bare triplet fullerene. It is a matter for further experimental and theoretical investigation to determine whether the lifetime of the triplet *c,c*-$C_{70}O$ oxidoannulene structure is long enough to enable measurement of a UV−vis spectrum and to determine how this spectrum might differ from its singlet counterpart.

Finally, isomer *a,b*-$C_{70}O_3$ has been shown experimentally to lead to *a,a*-$C_{70}O$, whereas *c,c*-$C_{70}O_3$ photolyses to a mixture of oxides. These results are more difficult to rationalize: the reactions are likely to run along one of a number of excited electronic state pathways, which may lead to the breaking of certain C−C bonds and thus force different dissociation channels to be favored.

IV. Conclusions

We have performed an extensive series of ab initio calculations to investigate why the *a,b*- and *c,c*-isomers of $C_{70}O$ are observed as final products in the fullerene ozonolysis reaction, when existing calculations in the literature have indicated that these structures do not represent the most stable structures. Our calculations have shown that the *a,b*- and *c,c*-isomers are the two most stable structures on the $C_{70}O_3$ PES, which strongly suggests that the reaction pathway toward oxide formation must proceed via the corresponding ozonide structure. Conversely,

the most stable oxide (*e,e*-) would originate from the least stable ozonide, which we offer as an explanation as to why this expected isomer has never been reported in the laboratory.

The energy barrier for the ozone ring-opening reaction is smallest for *e,e*-$C_{70}O_3$, and thus, we were able to observe it directly and spontaneously during the MD simulation. The process consists of breaking the C_e—C_e bond, followed by breaking one of the O—O bonds, which leads to a carbonyl and carbonyl oxide on the surface of the fullerene. The same mechanism is also valid for *a,b*- and *c,c*-$C_{70}O_3$, but because the reaction barriers are higher for these isomers, confirmation was obtained by transition-state searching. The calculated energy barriers thus obtained agreed well with values estimated from experiment.

The first two steps of the reaction we propose for the thermally induced decomposition of $C_{70}O_3$ are in agreement with the general mechanism for ozonolysis of alkenes proposed by Criegee. In addition to our calculations supporting this general mechanism, they also reveal the likely time scale of the reaction and indicate that it is the breaking of the C—C bond that triggers the whole process. We propose that, in further steps of the reaction, the molecule loses O_2 in its triplet or singlet electronic state and the O atom from the carbonyl group forms an oxygen bridge between the two neighboring nonbonded carbon atoms, thus leading to $C_{70}O$ in its triplet or singlet state, respectively. A pair of products initially in their singlet states seems to be more likely for the decomposition of *a,b*-$C_{70}O_3$, which ultimately leads to the closed *a,b*-$C_{70}O$ epoxide structure. For *c,c*-$C_{70}O_3$, it seems that the more thermodynamically favorable process is the one leading to dissociation products initially in their triplet electronic states. The *c,c*-$C_{70}O$ open oxidoannulene structure is expected, because it refers to the most stable minimum on the triplet PES of the *c,c*-isomer, which should subsequently decay to the stable epoxide singlet structure. Indeed, a metastable open structure was observed experimentally, which decayed photochemically to the final *c,c*-$C_{70}O$ epoxide structure, but it was ascribed by the authors to the *d,d*-$C_{70}O$ isomer. This work goes someway toward addressing the issues raised by Heymann and Weisman that more work is required to understand the nature of the PESs that give rise to the complicated net of observed reactions in the ozonolysis of fullerenes.

Finally, we note that the theoretical model implemented in our paper has some limitations that may influence the results. Due to the size of the fullerene molecule and the complexity of the chemical problem, the solvent has not been considered in our calculations. As the fullerene oxides and intermediates leading to them are slightly polar, interactions with solvent molecules may be an important factor influencing the mechanism of decomposition of fullerene ozonides.

Acknowledgment. This work has been performed under the HPC-EUROPA2 Project (Project number 228398) with the support of the European Commission Capacities Area, Research Infrastructures Initiative. A.B. would like to thank the Wroclaw Network and Supercomputing Center for access to computer time. C.A.M. acknowledges the Royal Society for the award of a University Research Fellowship. This work has made use of the resources provided by the EaSTCHEM Research Computing Facility (http://www.eastchem.ac.uk/rcf). This facility is partially supported by the eDIKT initiative (http://www.edikt.org). We thank Drs. Patricia Richardson and Andrew Turner (University of Edinburgh) for helpful discussions during the course of this work. The article is devoted to the memory of Professor Jan Łopuszański.

Supporting Information Available: Optimized bond lengths obtained for the parent C_{70} molecule, distances between the carbon atoms to which the oxygen atom is attached, and average C—C bond lengths observed in the MD simulation runs for the $C_{70}O_3$ series. This material is available free of charge via the Internet at http://pubs.acs.org.

References and Notes

(1) Diederich, F.; Ettl, R.; Rubin, Y.; Whetten, R. L.; Beck, R.; Alvarez, M. M.; Anz, S. J.; Sensharma, D.; Wundl, F.; Khemani, K. C.; Koch, A. *Science* **1991**, *252*, 548.
(2) Kroto, H. W.; Heath, J. R.; O'Brien, S. C.; Curl, R. F.; Smalley, R. E. *Nature* **1985**, *318*, 162.
(3) Heymann, D.; Weisman, R.B. C. R. *Chimie* **2006**, *9*, 1107.
(4) Heymann, D. *Fullerenes, Nanotubes and Carbon Nanostructures* **2004**, *12*, 715.
(5) Raghavachari, K. *Int. J. Mod. Phys. B* **1992**, *6*, 3821.
(6) Raghavachari, K.; Rohlfing, C. M. *Chem. Phys. Lett.* **1992**, *197*, 495.
(7) Wang, B.-C.; Chen, L.; Chou, Y.-M. *J. Mol. Struct. Theochem* **1998**, *422*, 153.
(8) D'yachkov, P. N.; Breslavskaya, N. N. *J. Mol. Struct. Theochem* **1997**, *397*, 199.
(9) Wang, B.-C.; Chen, L.; Lee, K.-J.; Cheng, C.-Y. *J. Mol. Struct. Theochem* **1999**, *469*, 127.
(10) Smith, A. B.; Strongin, R. M.; Brard, L.; Furst, G. T.; Atkins, J. H.; Romanow, W. J.; Saunders, M.; Jiménez-Vázquez, H. A.; Owens, K. G.; Goldschmidt, R. J. *J. Am. Chem. Soc.* **1996**, *61*, 1904.
(11) Bezmelnitsin, V. N.; Eletskii, A. V.; Scheptov, N. G.; Avent, A. G.; Taylor, R. *J. Chem. Soc., Perkin Trans.* **1997**, *2*, 683.
(12) Heymann, D.; Bachilo, S. M.; Weisman, R. B. *J. Am. Chem. Soc.* **2002**, *124*, 6317.
(13) Balch, A. L.; Costa, D. A.; Olmsted, M. M. *Chem. Commun.* **1996**, 2449.
(14) Lippert, G; Hutter, J.; Parinello, M. *Mol. Phys.* **1997**, *92*, 477.
(15) Vande; Vondele, J.; Krack, M.; Mohamed, F.; Parinello, T.; Chassaing, T.; Hutter, J. *Comput. Phys. Commun.* **2005**, *167*, 103.
(16) The CP2K developers group, http://cp2k.berlios.de/, 2008.
(17) Goedecker, S.; Teter, M.; Hutter, J. *Phys. Rev. B* **1996**, *54*, 1703.
(18) Ahlrichs, R.; Bär, M.; Häser, M.; Horn, H.; Kölmel, C. *Chem. Phys. Lett.* **1989**, *162*, 165.
(19) Deglmann, P.; Furche, F.; Ahlrichs, R. *Chem. Phys. Lett.* **2002**, *362*, 511.
(20) Deglmann, P.; Furche, F. *J. Chem. Phys.* **2002**, *117*, 9535.
(21) Helgaker, T. *Chem. Phys. Lett.* **1991**, *182*, 503–510.
(22) Schäfer, A.; Horn, H.; Ahlrichs, R. *J. Chem. Phys.* **1992**, *97*, 2571.
(23) Eichkorn, K.; Treutler, O.; Öhm, H.; Häser, M.; Ahlrichs, R. *Chem. Phys. Lett.* **1995**, *242*, 652.
(24) Bauernschmitt, R.; Häser, M.; Treutler, O.; Ahlrichs, R. *Chem. Phys. Lett.* **1997**, *264*, 573.
(25) Deglmann, P.; May, K.; Furche, F.; Ahlrichs, R. *Chem. Phys. Lett.* **2004**, *384*, 103.
(26) Rappoport, D.; Furche, F. *J. Chem. Phys.* **2005**, *122*, 064105.
(27) Flyvbjerg, H.; Petersen, H. G. *J. Chem. Phys.* **1989**, *91*, 461.
(28) Taylor, R. *J. Chem. Soc., Perkin Trans.* **1993**, *2*, 813.
(29) Criegee, R. *Angew. Chem., Int. Ed. Engl.* **1975**, *87*, 745.
(30) Geletneky, C.; Berger, S. *Eur. J. Org. Chem.* **1998**, 1625.
(31) Becke, A. D. *Phys. Rev. A* **1988**, *38*, 3098.
(32) Lee, C.; Yang, W.; Parr, R. G. *Phys. Rev. B* **1988**, *37*, 785.
(33) Becke, A. D. *J. Chem. Phys.* **1993**, *98*, 1372.
(34) Reed, A. E.; Weinstock, R. B.; Weinhold, F. *J. Chem. Phys.* **1985**, *83*, 735.
(35) Fraelich, M. R.; Weisman, R. B. *J. Phys. Chem.* **1993**, *97*, 11145.
(36) Etheridge, H. T.; Weisman, R. B. *J. Phys. Chem.* **1995**, *99*, 2782.

JP9024798